

Phenoxy imine NOON complexes of heavy alkaline earth ions for the ring-opening polymerisation of cyclic esters

Rebecca L. Jones, Zoë R. Turner, Jean-Charles Buffet and Dermot O'Hare*

Chemistry Research Laboratory, Department of Chemistry, University of Oxford, Mansfield Road, Oxford, OX1 3TA, United Kingdom. Tel: +44(0) 1865 285157; E-mail: dermot.ohare@chem.ox.ac.uk.

Table of Contents

I.	General considerations	S2
II.	Additional polymerisation data	S4
III.	References	S14

I. General considerations

All manipulations were carried out using standard Schlenk line or drybox techniques under an atmosphere of dinitrogen or argon. Protio solvents were degassed by sparging with dinitrogen, dried by passing through a column of activated sieves using an MBraun SPS-800 solvent purification system (pentane, hexane, toluene, benzene) and stored over potassium mirrors, or distilled from sodium metal (thf) and stored over activated 4 Å molecular sieves, or distilled from sodium-potassium alloy (diethyl ether) and stored over a potassium mirror. Deuterated solvents were dried over potassium (C_6D_6) or CaH_2 (C_4D_8O , $CDCl_3$), distilled under reduced pressure and freeze-pump-thaw degassed three times prior to use.

Solution NMR spectroscopy. Solution 1H NMR spectra were recorded at 298 K, unless otherwise stated, on Bruker AVIII 400 nanobay or Bruker AVIII 500 spectrometers and $^{13}C\{^1H\}$ or ^{13}C NMR spectra on the same spectrometers at operating frequencies of 100 and 125 MHz respectively. Two dimensional 1H - 1H and ^{13}C - 1H correlation experiments were used, when necessary, to confirm 1H and ^{13}C assignments. All NMR spectra were referenced internally to residual protio solvent (1H) or solvent (^{13}C) resonances and are reported relative to tetramethylsilane ($\delta = 0$ ppm). Chemical shifts are quoted in δ (ppm) and coupling constants in Hertz. Air sensitive samples were prepared in a glovebox under an inert atmosphere, using dried d

euterated solvents in J. Young's NMR tubes.

Fourier transform infrared (FTIR) spectroscopy. Fourier transform infrared (FTIR) spectroscopy samples were prepared in a glove box as pellets using anhydrous potassium bromide (KBr). IR spectra were recorded on a Nicolet iS5 ThermoScientific spectrometer (range = 4000 – 400 cm^{-1} with resolution = 1 cm^{-1}) in transmission mode. A background spectrum was run prior to the sample and was subtracted from the sample spectra.

Matrix Assisted Laser Desorption/Ionisation Time-of-Flight mass spectrometry (MALDI-ToF MS). Samples were prepared in a glove box under a nitrogen atmosphere and sealed in glass tubes. Samples were run as electron impact (EI) mass spectra on an Agilent GC-TOF-MS by Dr James Wickens or Dr Victor Mikhailov (University of Oxford).

Polymer tacticity analysis via $^1H\{^1H\}$ NMR spectroscopy. Polymer tacticity was analysed by $^1H\{^1H\}$ NMR spectroscopy. P_r values were calculated from the integrations obtained from the methine region of $^1H\{^1H\}$ NMR spectra. Alternatively, peak deconvolution, using the Mestrenova software package, was used to improve the accuracy of the determination.³⁷ The probability of a particular tetrad was then calculated using Bernoullian statistics.³⁸

Polymer end-group analysis via MALDI-TOF mass spectrometry. Polymer end group analysis was performed using Matrix-assisted laser desorption/ionisation time of flight spectra. Samples were prepared in chloroform at a concentration of 1 $mg\ mL^{-1}$ and filtered before analysis. MALDI-TOF spectra were collected Dr Victor Mikhailov (University of Oxford) using a Bruker MALDI Autoflex TOF MS. Samples were run using either a DHB or DCTB matrix. The DHB matrix was prepared by mixing the sample with DHB (10 $mg\ mL^{-1}$ in 70:30

H₂O:CH₃CN) in a 1:1 volume ratio. The DCTB matrix was prepared by mixing 10 μL of sample with 10 μL DCTB (40 mg mL⁻¹ in thf) and 2.5 μL KTFA (5 mg mL⁻¹ in thf). 1.5 μL of the mixed solutions were spotted on the MALDI plate and dried prior to the run.

Polymer molecular weight analysis via gel permeation chromatography (GPC). Polymer molecular weights and dispersities (M_n , M_w and $M_w/M_n = D$) were determined by GPC using a Polymer Laboratories PLGPC50 Plus instrument equipped with a Polymer Laboratories PLgel Mixed-D column (300 mm length, 7.5 mm diameter) and a refractive index (RI) detector. thf (Sigma Aldrich, HPLC grade) was used as an eluent at 30 °C with a flow rate of 1.0 mL min⁻¹. Samples were dissolved in thf at a concentration of 1.0 mg mL⁻¹ and filtered before injection. Linear polystyrenes were used as primary calibration standards and correction factor of 0.58 was applied to calculate the experimental molecular weights.³⁹

II. Additional polymerisation data

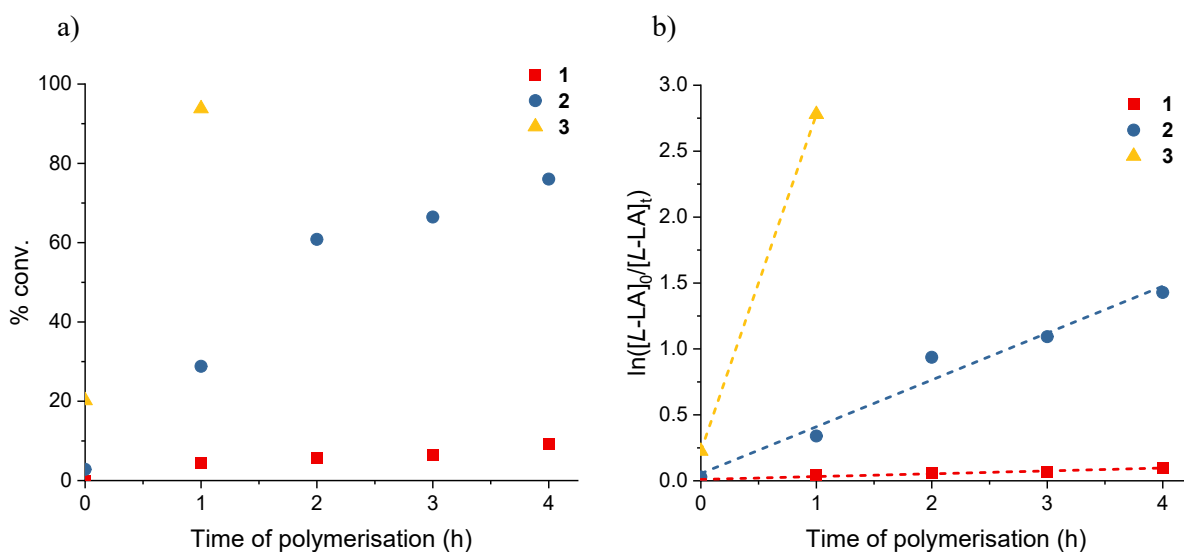


Fig. S1. a) Plots of percentage conversion vs. time. b) Plots of $\ln([L-LA]_0/[L-LA]_t)$ vs. time. Red squares: cat = **1** ($k_{\text{obs}} = 0.018 \text{ h}^{-1}$, $R^2 = 0.999$); blue circles: cat = **2** ($k_{\text{obs}} = 0.29 \text{ h}^{-1}$, $R^2 = 0.970$); yellow up triangles: cat = **3** (no k_{obs} or R^2 could be recorded). Conditions: $[L-LA]_0:[\mathbf{M}]_0 = 500:1$, $[L-LA]_0 = 0.5 \text{ M}$ in 0.6 mL benzene- d_6 at $40 \text{ }^\circ\text{C}$.

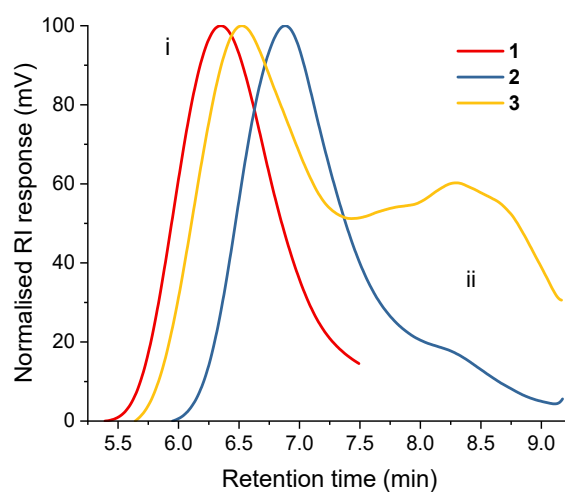


Fig. S2. GPC traces of PLAs synthesised from the ROP of *L*-LA. Red: cat = **1**, $M_n = 55\,276 \text{ g mol}^{-1}$, $\mathcal{D} = 1.59$; blue: cat = **2**, $M_n = 34\,403 \text{ g mol}^{-1}$, $\mathcal{D} = 1.69$; yellow: cat = **3**, $M_n = 40\,556 \text{ g mol}^{-1}$, $\mathcal{D} = 1.55$. Conditions: $[L-LA]_0:[\mathbf{M}]_0 = 500:1$, $[L-LA]_0 = 0.5 \text{ M}$ in 0.6 mL benzene- d_6 at $40 \text{ }^\circ\text{C}$. Analysis reported is of major peak i.

$$\mu\text{mol}_{\text{pol}} \div \mu\text{mol}_{\text{Ca}} = \frac{\text{chains}}{\text{metal}}$$

Equation S1

where $mol_{pol} = [\text{mass of LA used} \times \% \text{ conv.}] / M_{n,(\text{GPC})}$

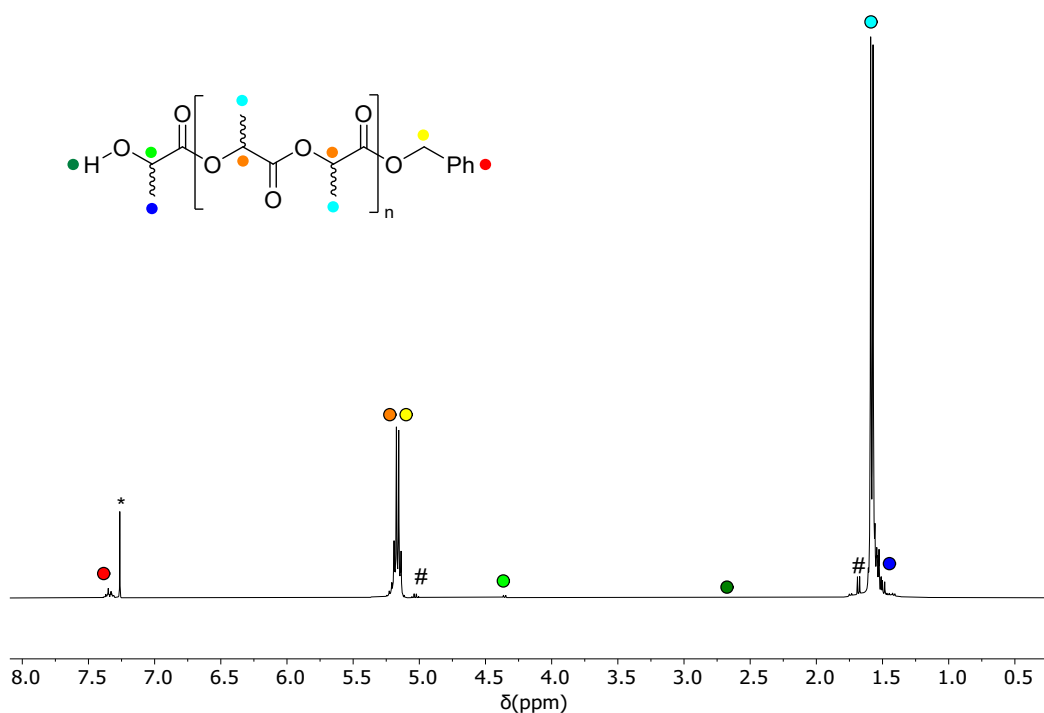


Fig. S3. ¹H NMR spectrum (*chloroform-*d*₁, 400 MHz, 298 K) of PLA produced using the 2/BnOH system. Polymerisation conditions: $[L\text{-LA}]_0:[\text{Sr}]_0:[\text{BnOH}]_0 = 500:1:1$, $[L\text{-LA}]_0 = 0.5 \text{ M}$, $0.6 \text{ mL benzene-}d_6$, $70 \text{ }^\circ\text{C}$, $D = 1.69$.

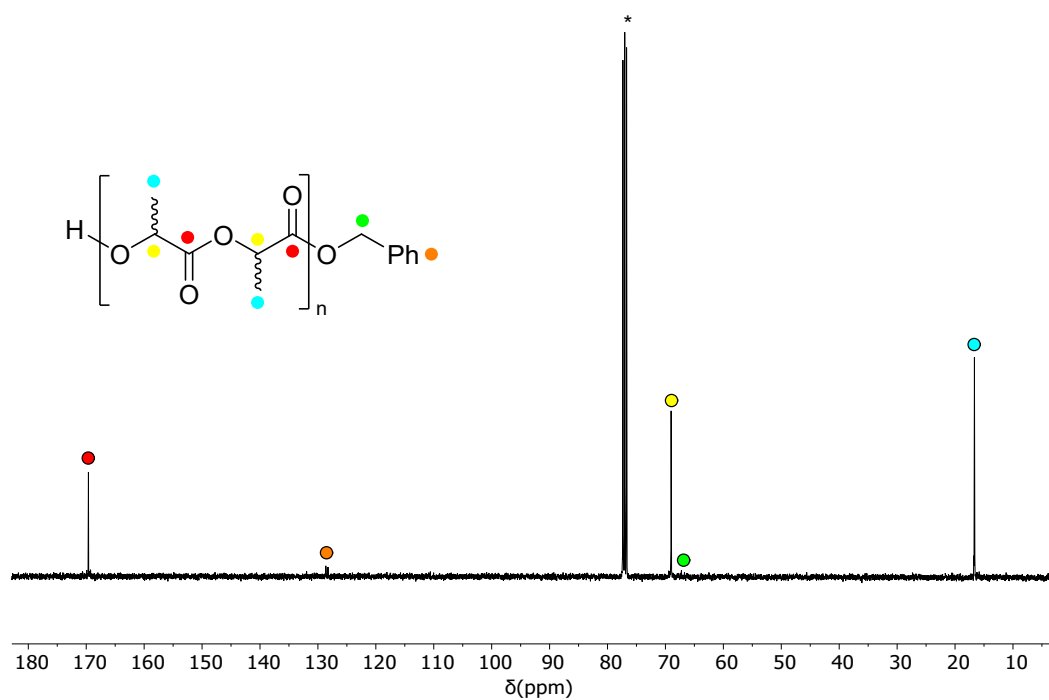


Fig. S4. $^{13}\text{C}\{^1\text{H}\}$ NMR spectrum (*chloroform- d_1 , 101 MHz, 298 K) of PLA produced using the **2**/BnOH system. Conditions: $[L\text{-LA}]_0:[\text{Sr}]_0:[\text{BnOH}]_0 = 500:1:1$, $[L\text{-LA}]_0 = 0.5$ M, 0.6 mL benzene- d_6 , 70 °C. , $D = 1.69$.

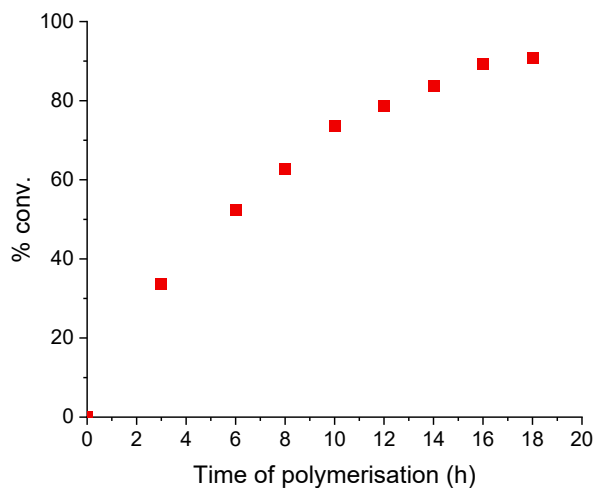


Fig. S5. Plot of percentage conversion to PLA as a function of time; reaction catalysed by the **1**/BnOH system. Conditions: $[L\text{-LA}]_0:[\text{Ca}]_0:[\text{BnOH}]_0 = 500:1:1$, $[L\text{-LA}]_0 = 0.5$ M in 0.6 mL benzene- d_6 at 40 °C.

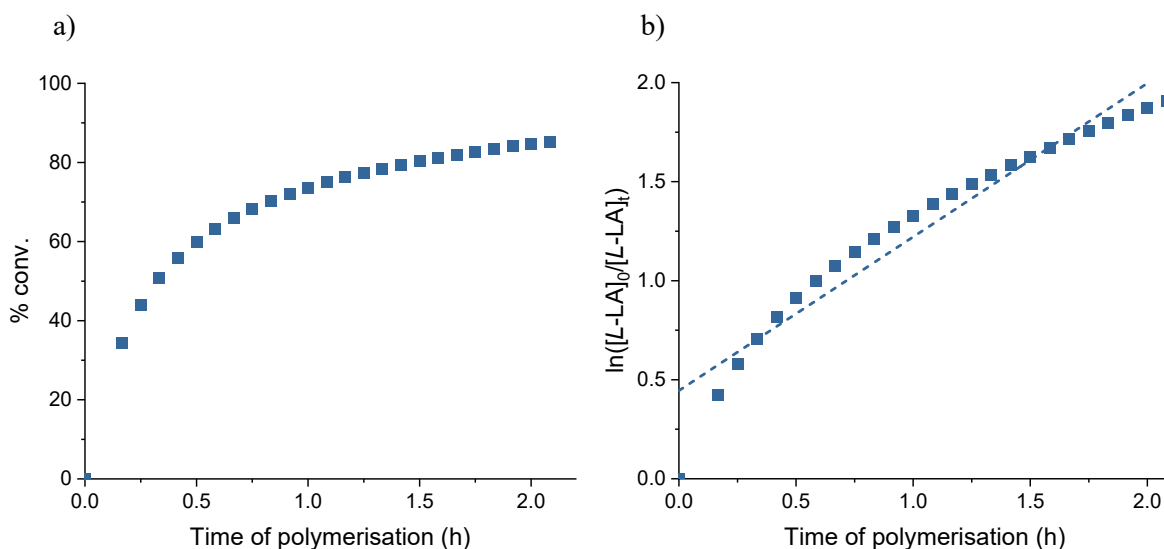


Fig. S6. a) Plot of percentage conversion to PLA as a function of time. b) Non-linear plot of $\ln([L\text{-LA}]_0/[L\text{-LA}]_t)$ vs. time for *L*-LA polymerisation using **2**/BnOH. Conditions: $[L\text{-LA}]_0:[\text{Sr}]_0:[\text{BnOH}]_0 = 500:1:1$, $[L\text{-LA}]_0 = 0.5$ M in 0.6 mL benzene- d_6 at 40 °C.

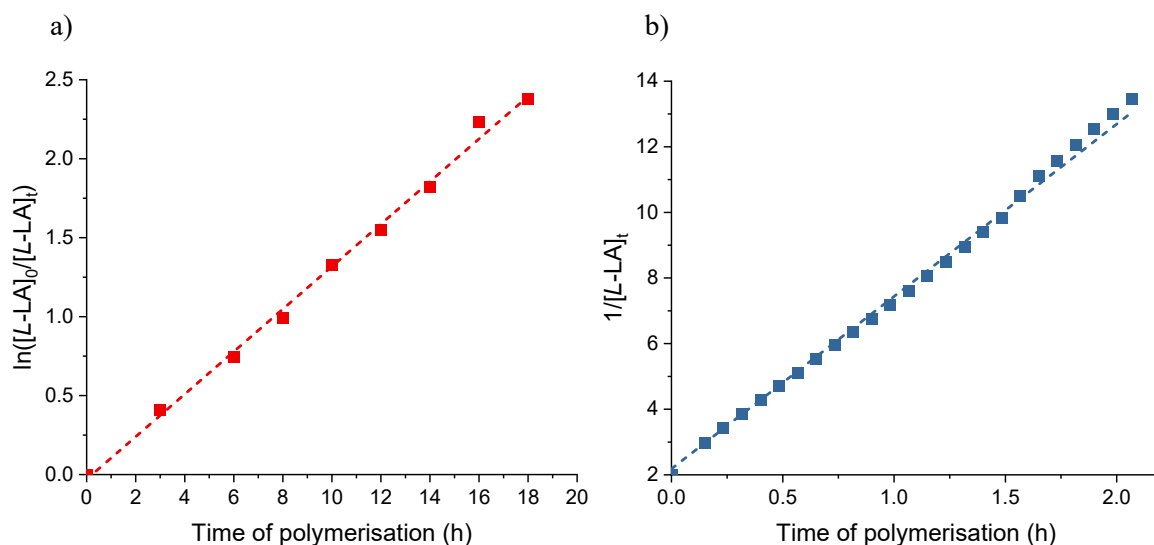


Fig. S7. a) Plot of $\ln([L-LA]_0/[L-LA]_t)$ vs. time for *L*-LA polymerisation using cat = **1**/BnOH ($k_{\text{obs}} = 0.14 \text{ h}^{-1}$, $R^2 = 0.992$). b) Plot of $1/[L-LA]_t$ vs. time for *L*-LA polymerisation using cat = **2**/BnOH ($k_{\text{obs}} = 5.30 \text{ M}^{-1} \text{ h}^{-1}$, $R^2 = 0.999$). Conditions: $[L-LA]_0:[\mathbf{M}]_0:[\text{BnOH}]_0 = 500:1:1$, $[L-LA]_0 = 0.5 \text{ M}$ in 0.6 mL benzene- d_6 at $40 \text{ }^\circ\text{C}$.

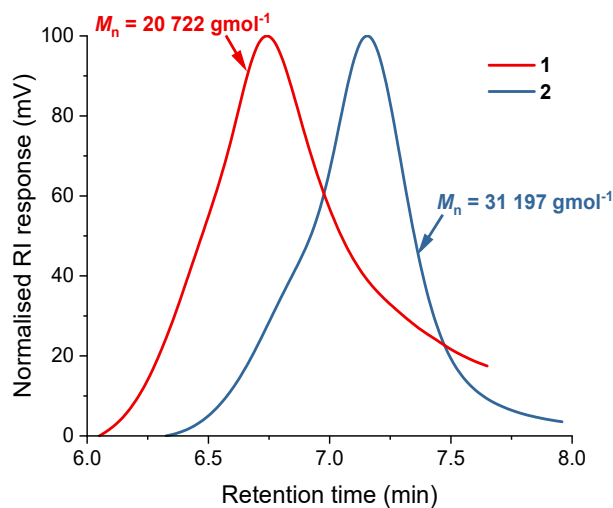


Fig. S8. GPC traces of PLAs synthesised from the ROP of *L*-LA. Red: cat = **1**/BnOH, $M_n = 20\,772 \text{ gmol}^{-1}$, $\mathcal{D} = 1.23$; blue: cat = **2**/BnOH, $M_n = 31\,197 \text{ gmol}^{-1}$, $\mathcal{D} = 1.38$. Conditions: $[L-LA]_0:[\mathbf{M}]_0:[\text{BnOH}]_0 = 500:1:1$, $[L-LA]_0 = 0.5 \text{ M}$ in 0.6 mL benzene- d_6 at $40 \text{ }^\circ\text{C}$.

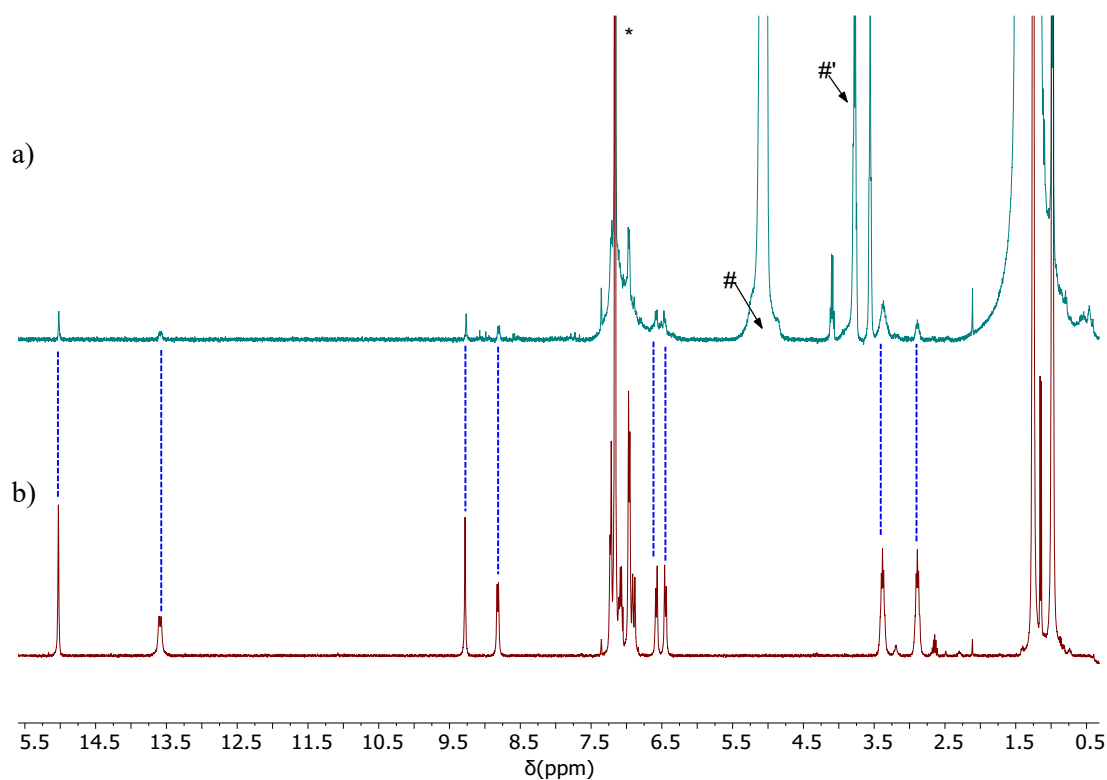


Fig. S9. ^1H NMR spectra (*benzene- d_6 , 400 MHz, 298 K) of a) an example polymerisation mixture and b) $\text{H}_2^{\text{DippL}}$. The presence of pro-ligand is highlighted by the blue dashed lines. # and #' represent PLA and LA respectively.

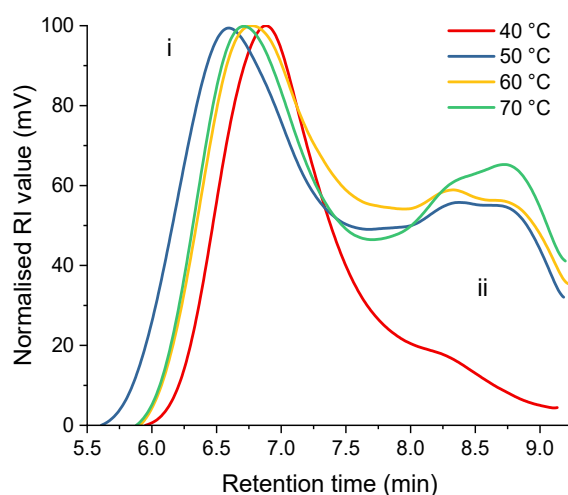


Fig. S10. Bimodal GPC traces of PLAs synthesised from the ROP of *L*-LA using **2**. Red: 40 °C, $M_n = 23\,766$ (i), 2401 (ii) g mol^{-1} , $D = 1.52$ (i), 1.39 (ii); blue: 50 °C, $M_n = 29\,961$ (**1**), 2001 (**2**) g mol^{-1} , $D = 1.68$ (i), 1.61 (ii); yellow: 60 °C, $M_n = 26\,468$ (i), 1888 (ii) g mol^{-1} , $D = 1.59$ (i), 1.67 (ii); green: 70 °C, $M_n = 31\,845$ (i), 1945 (ii) g mol^{-1} , $D = 1.56$ (i), 1.70 (ii). Conditions: $[L\text{-LA}]_0:[\text{Sr}]_0 = 500:1$, $[L\text{-LA}]_0 = 0.5$ M in 0.6 mL benzene- d_6 at stated temperature.

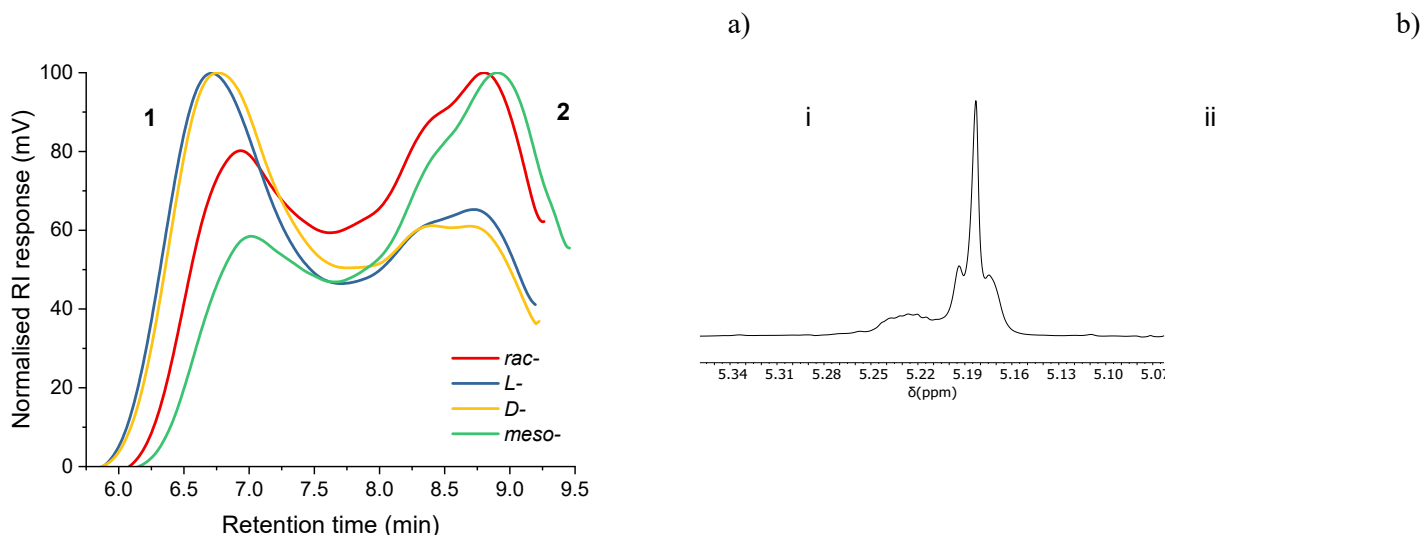


Fig. S11. a) Bimodal GPC traces of PLAs synthesised from the ROP of LA using **2**. Red: *rac*-LA, $M_n = 20\,871$ (i), 1625 (ii) g mol^{-1} , $\mathcal{D} = 1.59$ (i), 1.54 (ii); blue: *L*-LA, $M_n = 31\,845$ (i), 1945 (ii) g mol^{-1} , $\mathcal{D} = 1.52$ (i), 1.70 (ii); yellow: *D*-LA, $M_n = 26\,969$ (i), 1863 (ii) g mol^{-1} , $\mathcal{D} = 1.63$ (i), 1.56 (ii); green: *meso*-LA, $M_n = 19\,294$ (i), 1252 (ii) g mol^{-1} , $\mathcal{D} = 1.46$ (i), 1.73 (ii). Conditions: $[\text{LA}]_0:[\text{Sr}]_0 = 500:1$, $[\text{LA}]_0 = 0.5$ M in 0.6 mL benzene- d_6 at 70 °C. b) $^1\text{H}\{^1\text{H}\}$ NMR spectrum (chloroform- d_1 , 500 MHz, 298 K) of the methine protons in the PLA produced from the **2** system and *L*- or *D*-lactide. Conditions: $[\text{LA}]_0:[\text{Sr}]_0 = 500:1$, $[\text{LA}]_0 = 0.5$ M in 0.6 mL benzene- d_6 at 70 °C.

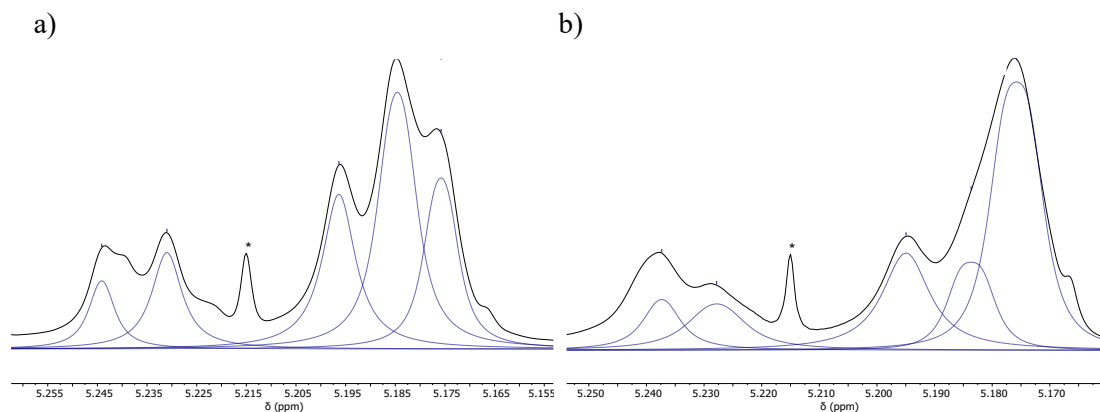


Fig. S12. a) $^1\text{H}\{^1\text{H}\}$ NMR spectra (chloroform- d_1 , 500 MHz, 298 K) of the methine protons in the PLA produced from the **2** system and a) *rac*-lactide ($P_m = 0.52$) and b) *meso*-lactide ($P_r = 0.74$). Conditions: $[\text{LA}]_0:[\text{Sr}]_0 = 500:1$, $[\text{LA}]_0 = 0.5$ M in 0.6 mL benzene- d_6 at 70 °C. * denotes an artefact from NMR “BASH” experiment set-up.

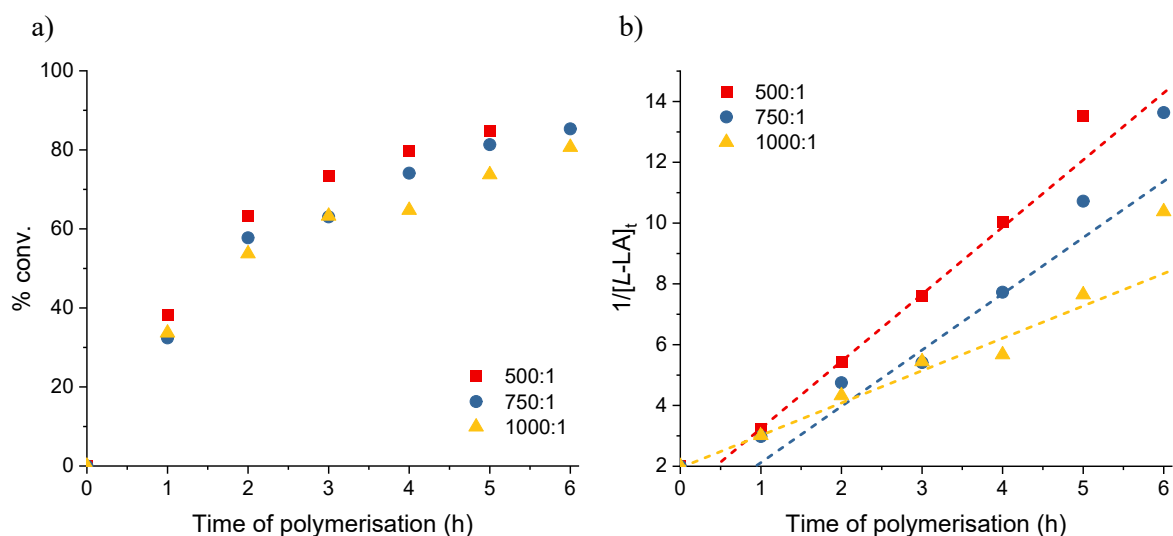


Fig. S13. a) Plots of percentage conversion vs. time. b) Plots of $1/[L-LA]_t$ vs. time for *L-LA* polymerisation using **2**. Red squares: 500:1 ($k_{\text{obs}} = 2.20 \text{ M}^{-1} \text{ h}^{-1}$, $R^2 = 0.999$); blue circles: 750:1 ($k_{\text{obs}} = 1.90 \text{ M}^{-1} \text{ h}^{-1}$, $R^2 = 0.948$); yellow up triangles: 1000:1 ($k_{\text{obs}} = 1.10 \text{ M}^{-1} \text{ h}^{-1}$, $R^2 = 0.970$). Conditions: $[L-LA]_0:[\text{Sr}]_0 = 500:1$, $[L-LA]_0 = 0.5 \text{ M}$ in 0.6 mL benzene- d_6 at $70 \text{ }^\circ\text{C}$.

Table S1. ROP of *L-LA* using **2** with $[L-LA]_0:[\text{Sr}]_0$ as stated in benzene- d_6 at $70 \text{ }^\circ\text{C}$.^a

$[LA]_0:$ $[Sr]_0$	Time (h)	Conv. (%) ^b	k_{obs} ($\text{M}^{-1} \text{ h}^{-1}$) ^c	R^2 ^c	M_n (GPC) ^d		M_n (calcd) ^g	\bar{D}		$H:L$ ^h
					i ^e	ii ^f		i ^e	ii ^f	
500:1	5	85	2.20 ± 0.01	0.999	31 845	1945	31 478	1.52	1.70	56:44
750:1	6	85	1.90 ± 0.3	0.948	32 806	1902	45 790	1.60	1.65	63:37
1000:1	6	81	1.10 ± 0.08	0.970	32 782	1828	58 913	1.73	1.53	67:33

^aConditions: $[L-LA]_0:[\text{Sr}]_0$ as stated, $[L-LA]_0 = 0.5 \text{ M}$ in 0.6 mL benzene- d_6 at $70 \text{ }^\circ\text{C}$.

^bAverage reported; measured by ^1H NMR spectroscopic analyses. ^cSecond-order rate constant (k_{obs}) and R^2 were obtained from average plots of $1/[L-LA]_t$ vs. time. ^dDetermined by GPC in thf against PS standards using the appropriate Mark-Houwink corrections.¹² ^eData corresponding to the higher molecular weight fraction. ^fData corresponding to the lower molecular weight fraction. ^gCalculated M_n for PLA synthesised (assuming two polymer chains propagate per metal centre) = $[(\text{conv.}(\%) \times [L-LA]_0/[\text{Sr}]_0) \times 144.13]/2$. ^hAverage higher:lower (H:L) molecular weight fraction ratio determined from area of peaks in average GPC trace.

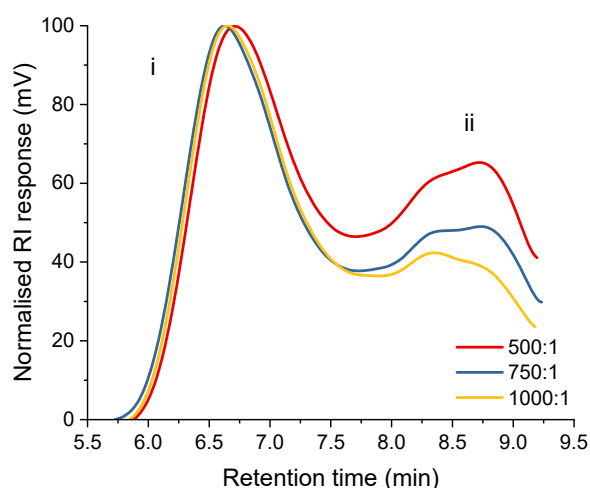


Fig. S14. Bimodal GPC traces of PLAs synthesised from the ROP of *L*-LA using **2**. Red: 500:1, $M_n = 31\,845$ (i), 1945 (ii) g mol^{-1} , $\mathcal{D} = 1.52$ (i), 1.70 (ii); blue: 750:1, $M_n = 32\,806$ (i), 1902 (ii) g mol^{-1} , $\mathcal{D} = 1.60$ (i), 1.65 (ii); yellow: 1000:1, $M_n = 32\,782$ (i), 1828 (ii) g mol^{-1} , $\mathcal{D} = 1.73$ (i), 1.53 (ii). Conditions: $[L\text{-LA}]_0:[\text{Sr}]_0$ as stated, $[L\text{-LA}]_0 = 0.5$ M in 0.6 mL benzene- d_6 at 70 °C.

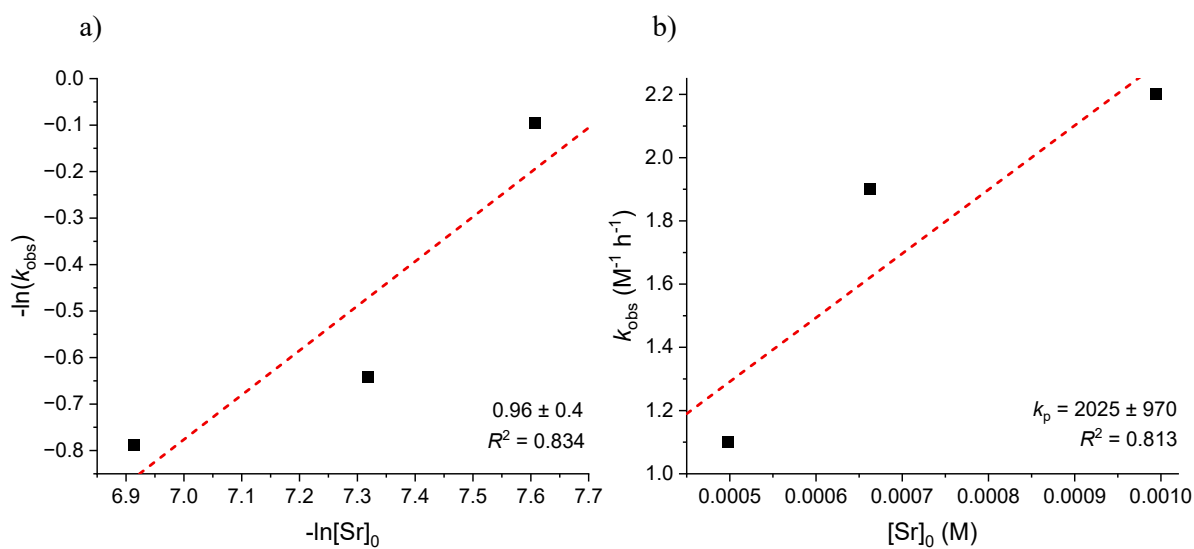


Fig. S15. a) Plot of $-\ln(k_{\text{obs}})$ vs. $-\ln[\text{Sr}]_0$ for ROP of *L*-LA using **2** shows that the order of reaction with respect to $[\text{Sr}]_0$ is equal to 0.96 ± 0.4 ; $R^2 = 0.834$. b) Plot of k_{obs} vs. $[\text{Sr}]_0$ for ROP of *L*-LA using **2** shows $k_p = 2025 \pm 970$ $\text{M}^{-1}\text{h}^{-1}$; $R^2 = 0.813$.

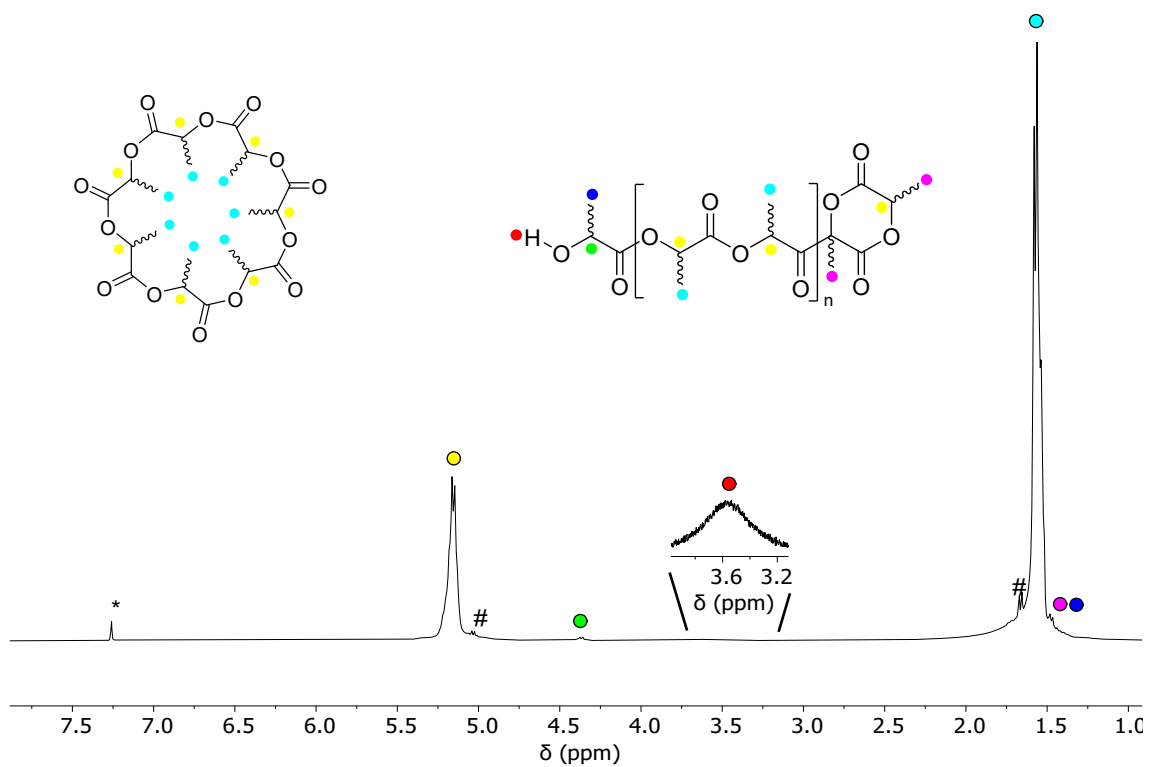


Fig. S16. ¹H NMR spectrum (*chloroform-*d*₁, 400 MHz, 298 K) of PLA produced using the **2** system. Conditions: $[L\text{-LA}]_0:[\text{Sr}]_0 = 500:1$, $[L\text{-LA}]_0 = 0.5$ M, 0.6 mL benzene-*d*₆, 40 °C., $D = 1.52, 1.39$. # represents residual monomer.

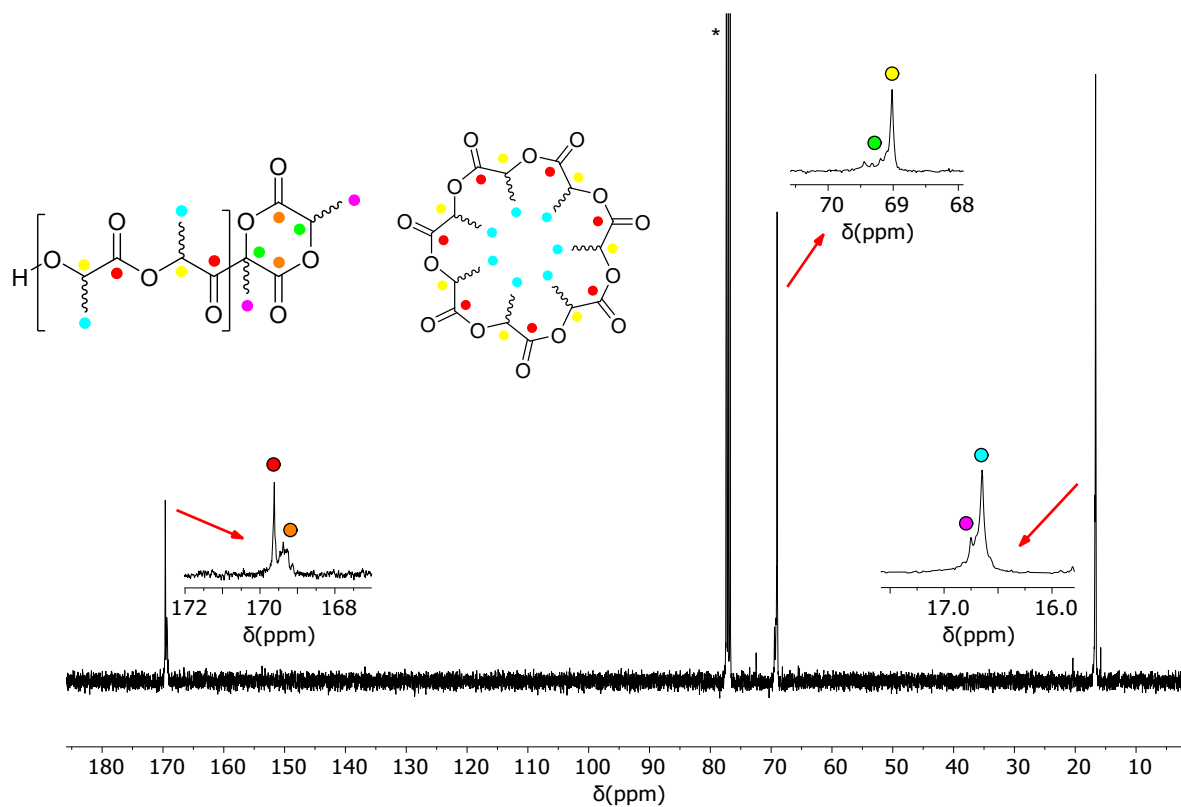


Fig. S17. $^{13}\text{C}\{^1\text{H}\}$ NMR spectrum (*chloroform- d_1 , 101 MHz, 298 K) of PLA isolated from a polymerisation catalysed by complex **2**. Conditions: $[L\text{-LA}]_0:[\text{Sr}]_0 = 500:1:1$, $[L\text{-LA}]_0 = 0.5$ M, 0.6 mL benzene- d_6 , 40 °C. , $D = 1.52, 1.39$.

III. References

- (1) Peng, C.-Y.; Shen, J.-Y.; Chen, Y.-T.; Wu, P.-J.; Hung, W.-Y.; Hu, W.-P.; Chou, P.-T. Optically Triggered Stepwise Double-Proton Transfer in an Intramolecular Proton Relay: A Case Study of 1,8-Dihydroxy-2-naphthaldehyde. *J. Am. Chem. Soc.* **2015**, *137* (45), 14349-14357. DOI: 10.1021/jacs.5b08562.
- (2) Salata, M. R.; Marks, T. J. Catalyst Nuclearity Effects in Olefin Polymerization. Enhanced Activity and Comonomer Enchainment in Ethylene plus Olefin Copolymerizations Mediated by Bimetallic Group 4 Phenoxyiminato Catalysts. *Macromolecules* **2009**, *42* (6), 1920-1933. DOI: 10.1021/ma8020745.
- (3) Sarazin, Y.; Howard, R. H.; Hughes, D. L.; Humphrey, S. M.; Bochmann, M. Titanium, zinc and alkaline-earth metal complexes supported by bulky O,N,N,O-multidentate ligands: syntheses, characterisation and activity in cyclic ester polymerisation. *Dalton Trans.* **2006**, (2), 340-350.
- (4) Cameron, T. M.; Xu, C.; Dipasquale, A. G.; Rheingold, A. L. Synthesis and Structure of Strontium and Barium Guanidinate and Mixed-Ligand Guanidinate Pentamethylcyclopentadienyl Complexes. *Organometallics* **2008**, *27* (7), 1596-1604. DOI: 10.1021/om701118j.
- (5) Cosier, J.; Glazer, A. M. A nitrogen-gas-stream cryostat for general X-ray diffraction studies. *J. Appl. Crystallogr.* **1986**, *19* (2), 105-107. DOI: doi:10.1107/S0021889886089835.
- (6) CrysAlisPRO, Oxford Diffraction /Agilent Technologies UK Ltd, Yarnton, England. (accessed).
- (7) Altomare, A.; Cascarano, G.; Giacovazzo, C.; Guagliardi, A. Completion and refinement of crystal structures with SIR92. *J. Appl. Crystallogr.* **1993**, *26* (3), 343-350. DOI: doi:10.1107/S0021889892010331.
- (8) Palatinus, L.; Chapuis, G. SUPERFLIP - a computer program for the solution of crystal structures by charge flipping in arbitrary dimensions. *J. Appl. Crystallogr.* **2007**, *40* (4), 786-790. DOI: doi:10.1107/S0021889807029238.
- (9) Farrugia, L. WinGX suite for small-molecule single-crystal crystallography. *J. Appl. Crystallogr.* **1999**, *32* (4), 837-838. DOI: doi:10.1107/S0021889899006020.
- (10) Spek, A. Single-crystal structure validation with the program PLATON. *J. Appl. Crystallogr.* **2003**, *36* (1), 7-13. DOI: doi:10.1107/S0021889802022112.
- (11) Farrugia, L. ORTEP-3 for Windows - a version of ORTEP-III with a Graphical User Interface (GUI). *J. Appl. Crystallogr.* **1997**, *30* (5 Part 1), 565. DOI: doi:10.1107/S0021889897003117.